

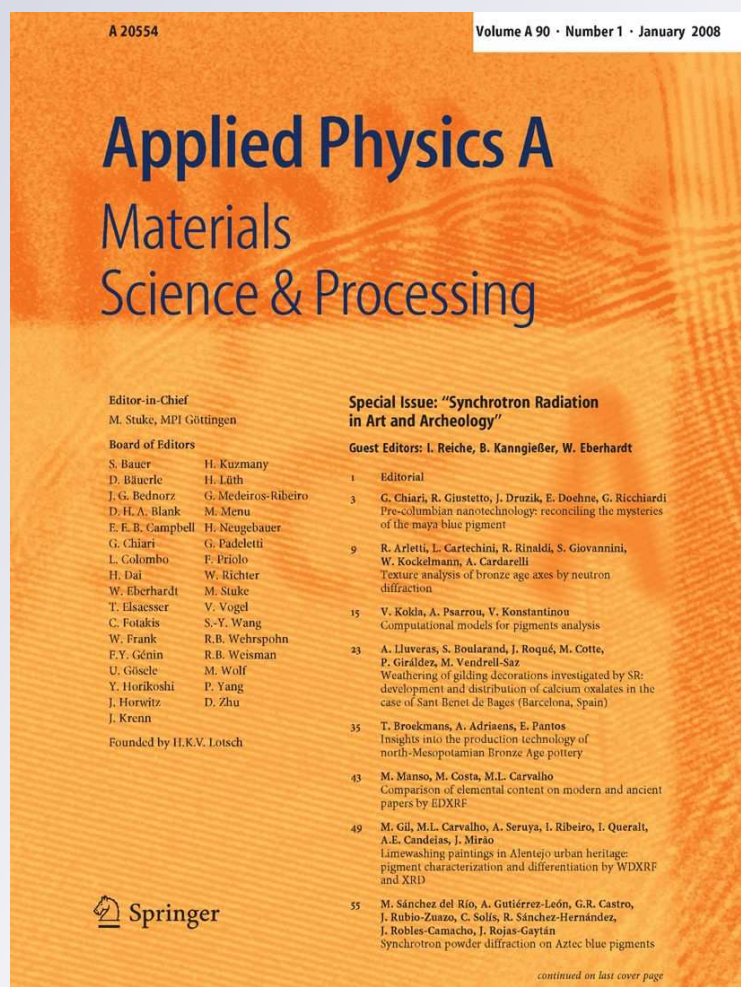
The formation of chlorine-induced alterations in daguerreotype image particles: a high resolution SEM-EDS study

*Silvia A. Centeno, Franziska Schulte,
Nora W. Kennedy & Alejandro G. Schrott*

Applied Physics A
Materials Science & Processing

ISSN 0947-8396

Appl. Phys. A
DOI 10.1007/s00339-011-6570-2



Your article is protected by copyright and all rights are held exclusively by Springer-Verlag. This e-offprint is for personal use only and shall not be self-archived in electronic repositories. If you wish to self-archive your work, please use the accepted author's version for posting to your own website or your institution's repository. You may further deposit the accepted author's version on a funder's repository at a funder's request, provided it is not made publicly available until 12 months after publication.

The formation of chlorine-induced alterations in daguerreotype image particles: a high resolution SEM-EDS study

Silvia A. Centeno · Franziska Schulte ·
Nora W. Kennedy · Alejandro G. Schrott

Received: 8 June 2011 / Accepted: 13 July 2011
© Springer-Verlag 2011

Abstract The daguerreotype image, composed of nano-sized silver–mercury or silver–mercury–gold amalgam particles formed on a polished silver substrate, is particularly sensitive to deterioration by chlorine-containing compounds resulting in the formation of AgCl that generates redeposited silver upon exposure to UV and visible lights. In the present study, alterations caused by chlorides on daguerreotype test samples prepared following 19th century recipes were studied. The dependence of variations in the production steps of daguerreotypes, such as multiple sensitization and gilding, on the impact of the exposure to chlorine were analyzed by scanning electron microscopy-energy dispersive X-ray spectrometry (SEM-EDS) and atomic force microscopy (AFM), complemented by X-ray fluorescence (XRF) and Raman spectroscopy. It was observed that AgCl nucleates on the image particles and in the substrate defects, regardless of the particle density or the sensitization process. In gilded samples, Au was observed over the image particles and the polished silver substrate as a tightly packed grainy layer, which

conformably follows the polishing irregularities. For the first time it is shown that Au preferentially accumulates on top of the image particles. This gold layer does not protect the image from chlorine-induced deterioration.

1 Introduction

The daguerreotype is one of the earliest photographic processes. It was disclosed in 1839 and was practiced extensively around the world until the early 1860s [1]. Introduced by Louis-Jacques-Mandé Daguerre [2], the original recipe starts with a polished silvered copper plate that is first sensitized with iodine vapors and then exposed to light in a camera. The latent image is developed with mercury vapors that condense preferentially in the areas struck by light, forming an amalgam with the silver. The resulting image is subsequently fixed by removing the unexposed silver salts and dried. A final step called gilding was later added to the original process in which a gold chloride solution was applied to the image before rinsing and drying [3]. Therefore, each daguerreotype is a unique positive having no negative from which to make second prints. Daguerreotypes amazed 19th century viewers as they do today with their rendering of portraits, landscapes, and other scenes, all with exquisite resolution and dynamic range [3, 4].

The daguerreotype image is composed of nanosized mercury–silver or mercury–gold–silver amalgam particles in the case of gilded plates, formed on a polished silvered copper substrate [3, 5]. The density and average size of the particles are directly related to the light exposure, with smaller particles and higher densities in the highlight areas. Barger et al. determined the average diameters of these particles to vary in gilded daguerreotypes from 0.1–1 μm to 0.25–2.5 μm for highlight and midtones, respectively, with

S.A. Centeno (✉) · F. Schulte
Department of Scientific Research, The Metropolitan Museum
of Art, 1000 Fifth Avenue, New York, NY 10028, USA
e-mail: silvia.centeno@metmuseum.org
Fax: +1-212-3965060

F. Schulte
George Eastman House, 900 East Avenue, Rochester, NY 14607,
USA

N.W. Kennedy
Photograph Conservation, The Metropolitan Museum of Art,
1000 Fifth Avenue, New York, NY 10028, USA

A.G. Schrott
IBM Research, Thomas J. Watson Center, Yorktown Heights,
NY 10598, USA

aggregates approximately 10–50 μm in the shadow areas. These authors reported particle diameters and densities of the same order of magnitude in non-gilded plates [3]. The unexposed areas appear black, whereas the particles in highlights and midtones cause diffuse scattering, with a fraction of the incident light directed back toward the viewer. The silver–mercury or silver–mercury–gold ratios in the image particles are not irrevocably resolved [3, 5, 6]. Barger et al. found varying ratios of these elements, not only for different plates but also for different image areas within the same plate, mainly using EDS [3].

To the present, there has not been agreement about the characteristics of the Au layer formed in the image during the gilding step. According to Swan et al., a Au layer approximately 0.75 μm thick covers both the image particles and the substrate [5], however, Barger et al. observed that Au accumulates preferentially in the high image density areas [3, 7]. More recently, Da Silva et al. concluded that Au is homogeneously distributed [8], while Ravines et al. reported that it only partially covers the image particles and the silver substrate [6].

The single sensitization process originally recommended by Daguerre involving iodine vapors required exposure times in the order of minutes that were impractical for portrait photography [3, 5]. Multiple sensitization processes were introduced by 1841 that lowered the exposure times to 20–40 seconds. In these processes, bromine, chlorine, or a combination, often with iodine, though bromine appears to have been the most common, were used after the first iodine sensitization step. And in 1847, a third sensitization step also involving iodine was added that allowed not only for shorter exposures but also to achieve a wider range of tones [5].

We have previously determined that some 19th century daguerreotypes are sensitive to ultraviolet and visible lights due to the presence of AgCl formed during exposure to chlorine-containing contaminants, as a result exhibition of these unique works has been dramatically curtailed over the last few years [9]. This form of deterioration appears as white deposits and/or white spots that partially obscure the image. In the white deposits and white spots, redeposited silver due to light exposure is present along with AgCl. Interestingly, the location of the white deposits and spots does not correlate with image features, such as highlights, midtones or shadows, and this suggests a complex deterioration mechanism to be elucidated. AgCl and Ag₂S are the corrosion products more frequently identified in silver objects exposed to the atmosphere [10]. AgCl can form through the reaction of elemental silver with gaseous chlorine, though the concentration of this gas in the atmosphere is very low, and by its reaction with HCl in humid environments; also the reaction of Ag with chloride-containing airborne particles has been frequently reported [10].

Over the decades, numerous methods have been employed in attempting to clean daguerreotypes of disfiguring tarnish. Many of these methods are now known to etch the plate, remove image particles, and leave behind chemical residues that can cause deterioration in various forms [3, 11]. Until the mid 1950s, the active ingredient of the most widely used cleaning solution was potassium cyanide. After this date, solutions of thiourea acidified with PO₄H₃ were in vogue [12]. It has also been suggested that before the introduction of PO₄H₃, thiourea solutions acidified with HCl or SO₄H₂, a formulation recommended for household silver cleaning, may have been used for treating daguerreotypes [3]. Thiourea has been recently demonstrated to partially remove the gold from the daguerreotype image [8]. Electro-cleaning [8], chemical sputtering [13], and laser cleaning [14, 15] have been proposed within recent decades for removing tarnishing layers and debris from daguerreotypes. Ultimately, the development of safe conservation treatments and suitable preservation strategies can only be done on the basis of an in-depth understanding of the different image deterioration mechanisms.

To study the formation of AgCl in the daguerreotype image, and to determine how variations in the manufacturing process determine the impact of the exposure to chlorine-containing compounds, samples that mimic pristine 19th century daguerreotypes were used. A gilded daguerreotype by an unknown artist dating from the 19th century was characterized under identical conditions as those used for the laboratory samples in order to determine whether the laboratory samples are suitable systems for mimicking the deposition of chlorine in original artworks.

2 Experimental

2.1 Samples

The samples used for the present study comprise a historic daguerreotype dating from the 19th century and daguerreotype step tablets made by Mike Robinson (Century Darkroom, Toronto) following the methodology described by Humphrey [16]. For the latter, silvered copper plates prepared by the traditional clad rolling method, in which the copper sheet has a thickness of approximately 480 μm and the Ag layer is between 16 and 25 μm , were used. These plates were first hand polished and subsequently re-silvered by immersing them in a bath containing sodium thiosulfate and AgCl, the latter prepared by mixing AgNO₃ and NaCl, and then repeatedly washed with distilled water before sensitization. A set of samples was sensitized with I₂ for 90 seconds, and another set was exposed to a multiple sensitization process, I₂/Br₂/I₂, for a total of 175 seconds. Three different light exposures were used in order to obtain

high, medium, and low image density areas in step tablets. The images were developed with mercury vapors at 70°C for eight minutes and subsequently fixed with a 3% sodium thiosulfate solution. A set of samples was gilded using a 0.1% $\text{HAuCl}_4 \cdot x\text{H}_2\text{O}$ solution, containing 0.8% of sodium thiosulfate. The gilding solution was poured over the image and the plate was lightly heated with an alcohol lamp for approximately 60 seconds. A similar set of step tablets was left ungilded. After the final step, the samples were washed thoroughly with water, dried with hot air and stored in a nitrogen atmosphere to avoid tarnishing. Each set of step tablets was prepared from a single full plate and was cut to size after the full daguerreotype process was completed to ensure homogeneity.

Chlorine was deposited by placing the step tablets over a saturated NaCl solution in a desiccator for three weeks or by dipping them in a 10% aqueous NaClO solution for two to three seconds. All the samples exposed to chlorine-containing compounds were stored in the dark in a nitrogen atmosphere to avoid light-induced changes or further tarnishing.

2.2 SEM/EDS and AFM

Scanning electron microscopy (SEM) images were acquired with a Carl Zeiss Ultra scanning electron microscope. The accelerating voltage was 2–10 KeV for the acquisition of high resolution images and 0.8 eV for obtaining compositional information, in the latter case using the Energy and angle selective Backscattered (EsB) detector. EDS spectra were acquired with an accelerating voltage of 15 KeV, therefore a contribution of the substrate to the Ag signal was expected when the image particles were analyzed. When not indicated, the images shown were acquired with the SEM in-lens detector. Atomic force microscopy (AFM) measurements were performed with a Digital Instruments Nanoscope IIIa.

2.3 XRF spectroscopy

For the X-ray fluorescence spectroscopy (XRF) measurements, a Bruker Artax μ -XRF spectrometer equipped with a Rh excitation tube and a Peltier-cooled silicon drift detector was used. The operating parameters for the tube voltage and anode current were set at 50 kV and 0.7 mA, respectively. A collimator was used resulting in a beam diameter of 600 μm . The different spots in the samples and the historic daguerreotype were analyzed for a 200 s live-time. For the mapping measurements, a 0.5 mm step width was chosen and ten measurements were performed in the horizontal direction and eleven spectra were acquired along the vertical direction. The acquisition live-time for each spectrum was 70 s.

2.4 Raman spectroscopy

Raman spectroscopy measurements were carried out with a Renishaw System 1000 coupled to a DM LM Leica microscope. Spectra were recorded by focusing a 785 nm laser (Spectra Physics, Irvine, USA) beam using a 50 \times objective lens. Neutral density filters were used to set the laser power at the sample to values between 0.2 and 1.5 mW. A 1200 lines/mm grating and a thermoelectrically cooled CCD detector were used, with integration times of 10–40 s.

3 Results and discussion

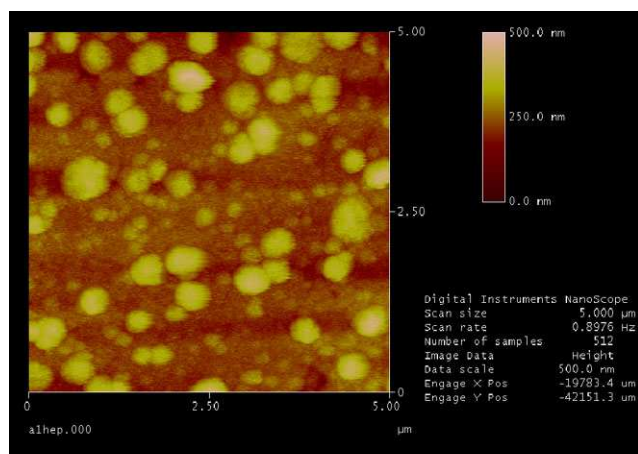
3.1 Analysis of untreated daguerreotype samples and of a 19th century plate

The approximate image particle diameters and surface densities, as determined by scanning electron microscopy (SEM) and atomic force microscopy (AFM), in the high-light, midtone, and low image density areas of the daguerreotype step tables prepared following a 19th century recipe were found to be within the ranges of those reported by Barger et al. for gilded and non-gilded historic daguerreotypes [3]. However, our AFM experiments more precisely showed a bimodal distribution of diameters and heights in the high image density regions (Fig. 1a). In contrast, the medium density areas yielded a distribution of predominantly larger particles and more uniform heights (Fig. 1b).

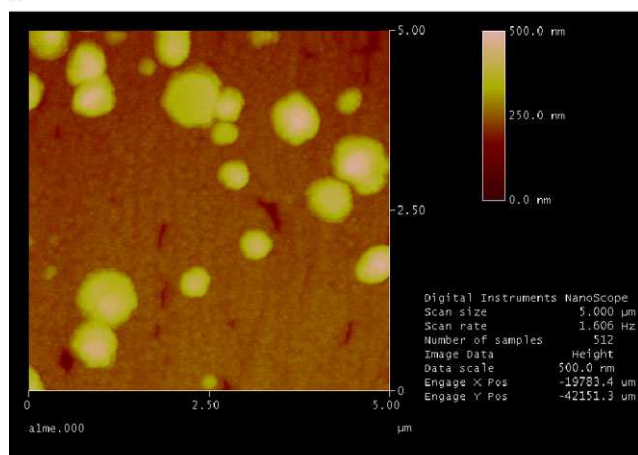
As for the influence of the sensitization on the particle size, it was observed that the average particle was larger when a three step process ($\text{I}_2/\text{Br}_2/\text{I}_2$) was used, particularly in the lower image density areas, when compared to samples prepared with a single sensitization step. These results are shown for non-gilded and gilded samples in Figs. 2a–2d.

As mentioned above, to the present date, there has not been consensus about the characteristics of the Au layer formed in the gilding step. In Figs. 2b and 2d, SEM images of gilded samples prepared using single and multiple sensitization processes, respectively, are shown, where it can be observed that a granular layer uniformly covers the surface of the daguerreotype in the gilded samples, conformably following the surface irregularities such as the polishing marks. The gilding layer also covers the image particles that appear more round when compared to the image particles in the non-gilded samples. AFM measurements carried out in these gilded samples (not shown) gave similar particle size and height distributions as those observed for the non-gilded samples shown in Figs. 1a and 1b. However, the image particles in all the gilded samples are approximately 300 nm higher, as measured by AFM, suggesting that the Au accumulates preferentially on top of the image particles.

A previous study of a gilded 19th century daguerreotype reported that Au does not completely cover the image



a



b

Fig. 1 AFM images acquired in a high (a) and medium image density (b) areas, respectively, of a non-gilded daguerreotype sample prepared using a single sensitization step with I_2

particles nor the silver substrate [6]. It is possible that in some historic plates past conservation treatments have partially removed the Au layer. The main advantage of using samples made under well controlled conditions is that they do not suffer from the uncertainties of historic daguerreotypes, most of which have been subjected to extremely invasive conservation/restoration treatments in the past or kept in non-controlled environments [3, 8, 9, 11–13]. For example, as mentioned above, thiourea cleaning solutions have been recently demonstrated to partially remove the Au from daguerreotype images [8].

Even though the Au layer uniformly covers the daguerreotype image, the total amount of Au deposited is not constant for the different image density areas. X-ray fluorescence (XRF) mapping experiments performed in the step tablets showed that Au preferentially accumulates in the high image density areas (maps not shown). We have recently reported a similar correlation between image density and Au content in a daguerreotype dating from ca. 1850

when adjacent areas with different image densities were included in the XRF map [17]. These results are also in agreement with the AFM measurements discussed above that showed that Au accumulates preferentially on top of the image particles. This is probably due to the higher affinity of Au for Hg, which is present only in the image particles.

A daguerreotype by an unknown artist dating from the 19th century (Fig. 3a) was first analyzed by XRF and determined to be gilded. The plate was then examined by SEM under identical experimental conditions as those used for the experimental step tablets in order to compare and determine whether the laboratory samples are suitable systems for mimicking the deposition of chlorine in real artworks. An SEM image acquired in a high image density area in this historic daguerreotype is presented in Fig. 3b, where it can be observed that the approximate image particle size and shape as well as the morphology and uniformity of the Au layer are similar to those in the gilded step tablets (Fig. 2b).

3.2 Analysis of daguerreotype samples exposed to chlorine-containing compounds

Daguerreotype step tablets kept in a desiccator over a saturated NaCl solution showed a white deposit after three weeks of treatment, and samples dipped into a 10% NaClO solution presented visible signs of deterioration after two to three seconds. In samples subjected to both treatments, AgCl was identified by its characteristic Raman band at ca. 240 cm^{-1} [18] (spectra not shown). This peak was observed in Raman spectra taken in areas showing a white deposit, particularly in the edges, as well as in the center of the samples, where no white deposit was visible to the naked eye. The sensitive detection of AgCl using Raman spectroscopy is due to the fact that the nanosized image particles behave as a surface enhanced Raman scattering (SERS) substrate [9]. This increased sensitivity allows to detect chlorine in amounts that are below the detection limit of XRF, a technique routinely used to analyze works of art in a non-invasive manner. However, it has to be kept in mind that the Raman signal intensity will be determined in part by the properties of the nanostructured metal surface [19]. The microstructures of areas with different image density or the changes that occur when the images are exposed to UV or visible light will lead to different enhancement factors. We have observed that the Ag–Cl characteristic bands are more intense in areas of artistic daguerreotypes where Ag redeposition has taken place due to exposure to UV and/or visible light [9], therefore the intensity of the band at ca. 240 cm^{-1} cannot be used to estimate the amount of chloride deposited.

Figures 4a and 4b show SEM images acquired in the same highlight area of a non-gilded daguerreotype step

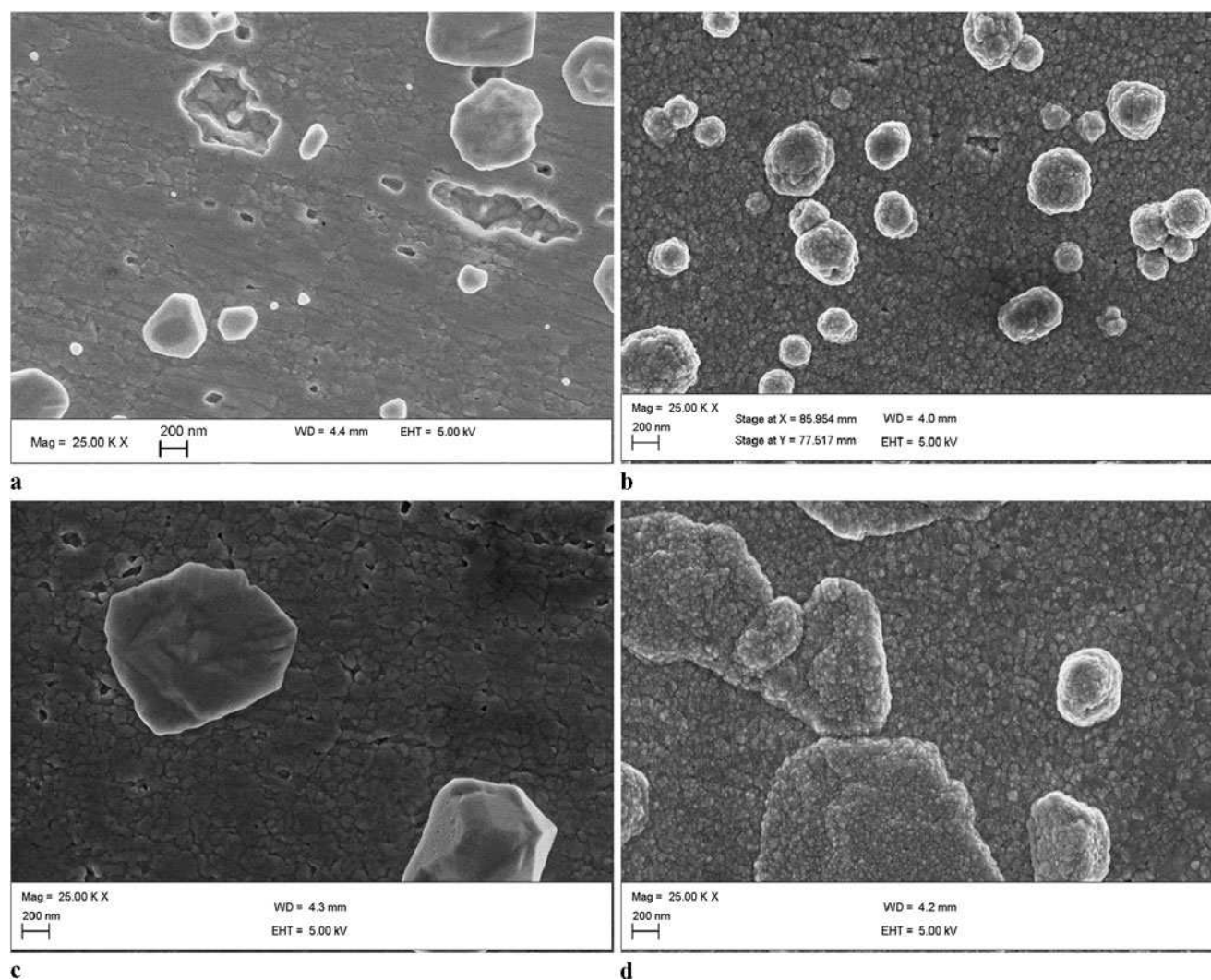


Fig. 2 SEM images of midtone areas in non-gilded (a) and gilded (b) daguerreotype samples, respectively, prepared using a single sensitization step with I_2 ; (c) and (d) correspond, respectively, to midtone areas of non-gilded and gilded samples sensitized with $I_2/B_2/I_2$

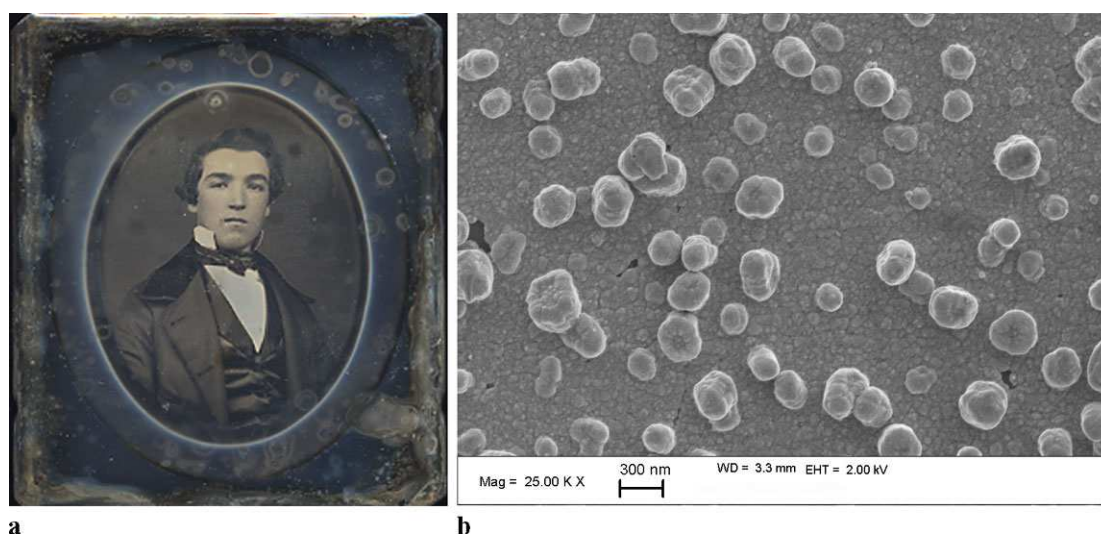


Fig. 3 (a) Gilded daguerreotype dating from the 19th century and depicting the portrait of an unknown man. (b) SEM image acquired in the man's shirt area (highlight)

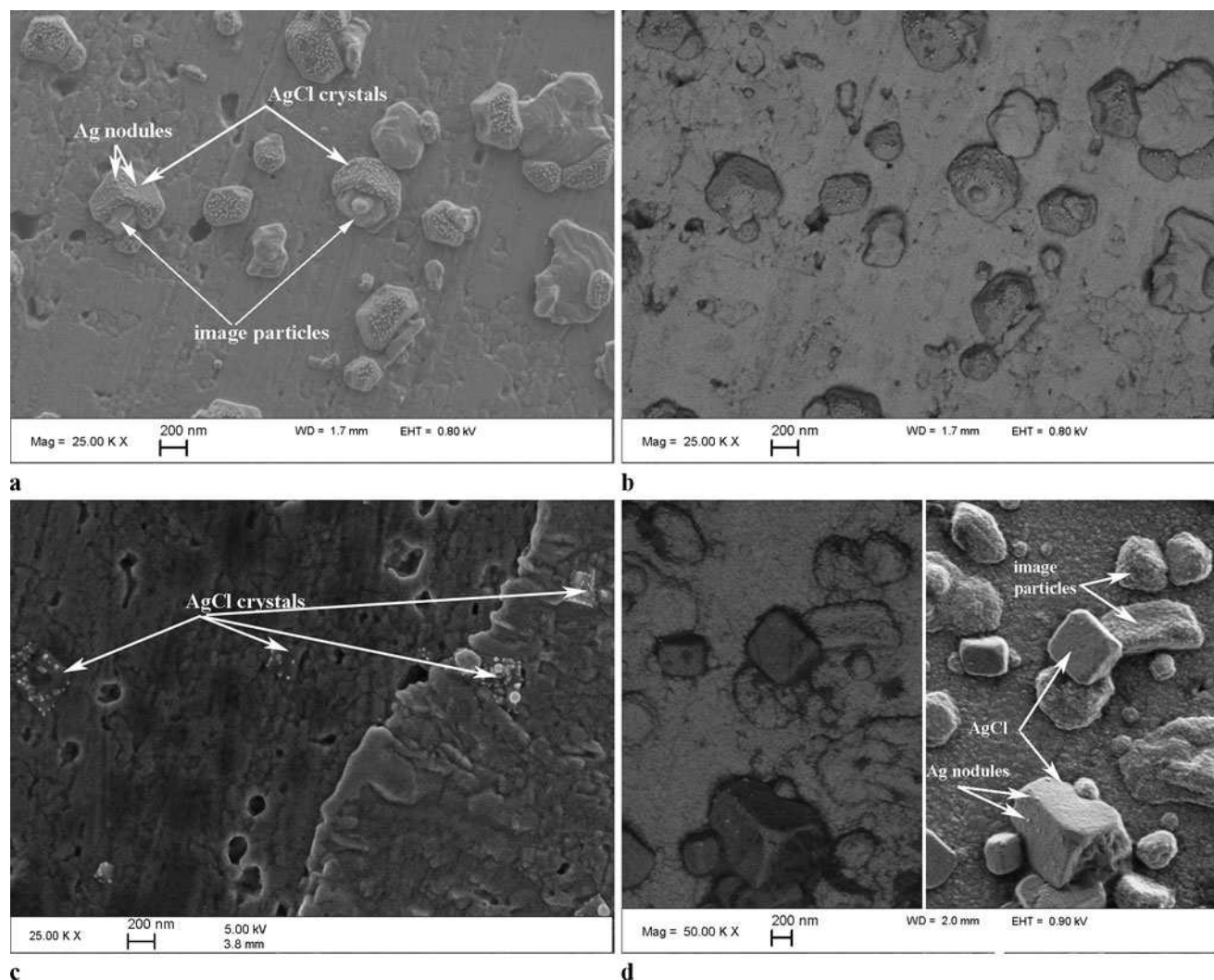


Fig. 4 SEM images of daguerreotype samples exposed to NaCl in a desiccator for three weeks: **(a)** and **(b)** correspond to the same highlight area in a non-gilded sample sensitized with $I_2/B_2/I_2$, acquired with the In-lens and EsB detectors, respectively; **(c)** was taken in the low image density area of the same step tablet shown in **(a)** and **(b)**; **(d)** SEM image of a highlight area in a gilded step tablet sensitized with $I_2/B_2/I_2$, acquired with the EsB detector (*left*) and with the In-lens detector (*right*), respectively

tablet prepared using a multiple sensitization process and exposed to NaCl in a desiccator for three weeks. In these figures, cubic AgCl crystals that have nucleated on image particles are clearly visible. Figure 4a shows the high resolution image formed by the in-lens detection of the elastically backscattered electrons (EBSE). Figure 4b shows an image formed by the EsB detector, which optimizes the detection of high angle backscattered electrons carrying an energy close to the landing energy of the primary beam (BSE), and exhibits nanoscale compositional information. In this case, the contrast is given by the metallic (brighter) areas and the insulating (darker) particles. The lower brightness of the latter obeys the fact that the band-gap of the insulating material limits the available channels for generating BSEs.

In Fig. 4c, an SEM image taken in the low image density area of the same step tablet presented in Figs. 4a and 4b

shows that AgCl can also nucleate in the defects of the polished silvered copper substrate. The fact that AgCl can nucleate both in image particles and in the substrate defects explains why the location of the white deposit and white spots in deteriorated 19th century daguerreotypes does not correlate with the location of image features such as highlights, midtones or shadow areas.

AgCl was also found to nucleate in gilded samples, as shown in Fig. 4c, indicating that the Au layer, even if it is in good condition and it has not been abraded or partially removed, does not protect the image from chlorine-induced deterioration.

The composition of the cubic crystals formed in the samples exposed to chlorine-containing compounds was confirmed as AgCl by EDS. An EDS line scan acquired in a gilded sample exposed to NaCl, in which the composition

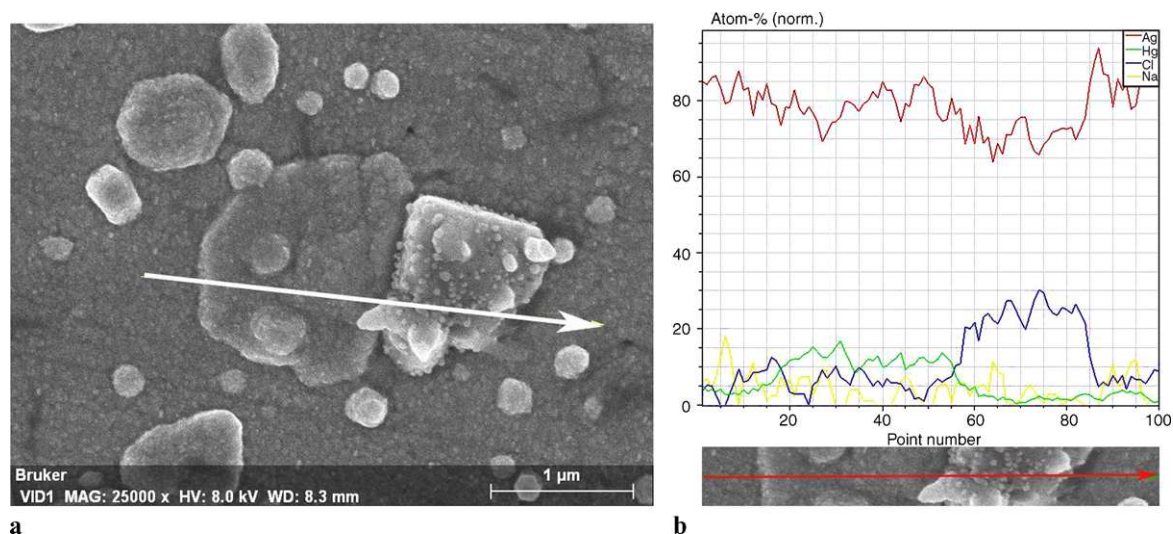


Fig. 5 (a) SEM image and (b) EDS line scan showing the distribution of Ag, Hg, Cl and Na across an image particle and a AgCl crystal in a gilded sample prepared using a multiple sensitization process with $I_2/B_2/I_2$, and exposed to NaCl in a desiccator for three weeks

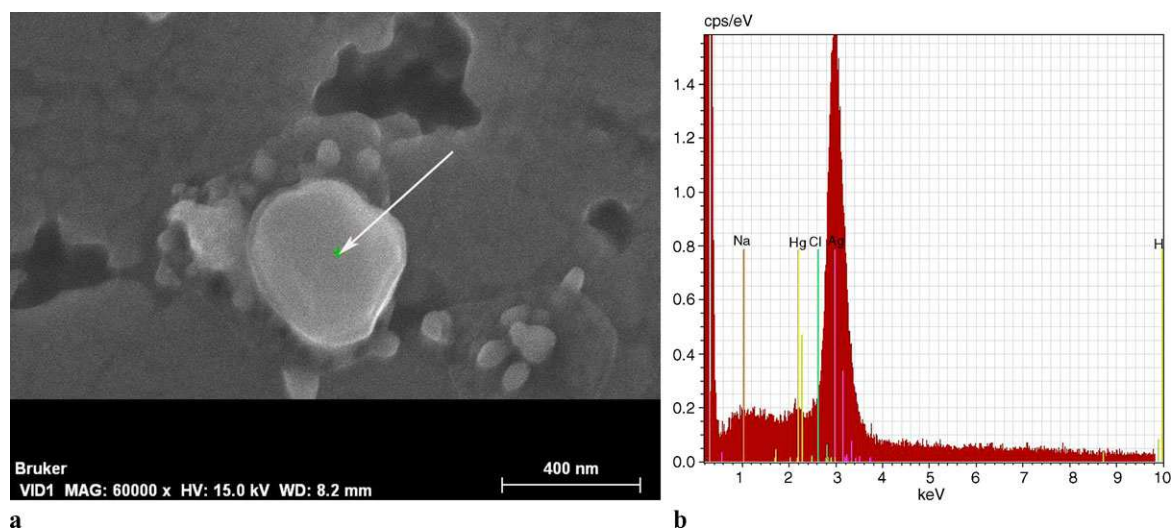


Fig. 6 (a) SEM image of a Ag nodule formed in a AgCl crystal that nucleated in a low image density area of a non-gilded daguerreotype sample. (b) EDS spectrum acquired in the spot indicated in an arrow in (a), 15 KeV

of a cubic crystal that has nucleated over an image particle is shown to be AgCl, is presented in Fig. 5b along with the corresponding SEM image in Fig. 5a.

When the image areas treated with chlorides are exposed to the electron beam in the SEM, silver nodules are formed on the surface of the AgCl crystals within seconds, both in gilded and in non-gilded samples. These silver nanoparticles are clearly visible in Figs. 4a–4d and 5a. The composition of said nodules was determined by exposing a region for several minutes to allow for nucleation and growth of a nodule of sufficient size to allow compositional determination. In Fig. 6, the composition of a nodule approxi-

mately 400 nm in diameter, formed in a AgCl crystal is confirmed as Ag by EDS. The formation of silver nanodots on Ag₂S upon interaction with the electron beam has been previously reported [20]. As mentioned above, UV illumination of chlorine-containing white deposits formed on daguerreotypes causes the formation of metallic silver that further alters the visual appearance of the images within a second. In addition, AgCl present in daguerreotype images is sensitive to visible illumination. This may be explained by Ag clusters that are able to shift the photoactive range of AgCl into the visible [21], but also by the presence of impurities such as silver sulfide, silver oxide, and cuprous ions, all frequently

detected in historic daguerreotypes [3], which confer photosensitivity to AgCl [22].

4 Conclusions

SEM-EDS analysis of a gilded 19th century daguerreotype showed that the image particle morphology and approximate size, as well as the characteristics of the gilding layer, are similar to those observed in the samples prepared for the present study following 19th century recipes and, therefore, that the latter are suitable systems for mimicking the deposition of chlorides in real artworks.

We characterized these test samples before and after exposure to chlorine using high resolution SEM and AFM complemented by Raman spectroscopy and XRF mapping. Before exposure to chlorine, the samples exhibited bimodal particle size and height distributions in the high image density areas, and a predominantly larger particle sizes in the medium density areas. Previous studies using SEM imaging only refer to particle size ranges, without specifying a size distribution. We also characterized the properties of the Au layer formed during the gilding step using these techniques. In all the image areas, high, medium and low density, Au is observed over the polished silver substrate and the image particles as a continuous grainy layer, with larger amounts present on top of the image particles.

In the samples exposed to chlorine, we observed that AgCl nucleates not only on the nanosized image particles but also in the substrate defects, regardless of the particle density or the sensitization process, explaining why the location of the white deposits formed in 19th century daguerreotypes that have been exposed to chlorine contamination does not correlate with the location of image features. The Au layer formed during the gilding step does not protect the daguerreotype image from chlorine-induced deterioration, even if this layer is in good condition and has not been partially removed. Silver nodules were observed on the AgCl crystals after a few seconds of exposure to the electron beam in the SEM, both in the gilded and non-gilded samples.

Acknowledgements The authors would like to thank Ralph Wiegandt and Taina Meller from the George Eastman House International Museum, Patrick Ravines from the Art Conservation Program at Buffalo State College, and Annette Manick from the Museum of Fine Arts Boston for helpful discussions. We are also grateful to Tony Frantz, Federico Caró, Mark T. Wypyski and Marco Leona at the Metropolitan Museum for sharing their expertise. We are indebted to Mike Robinson of Century Darkroom in Toronto, Canada, for his careful work in the preparation of the step tablets and to Peter Mustardo, from The Better Image, for lending the 19th century TBI Study Collection daguerreotype for analysis. We gratefully acknowledge the generous financial support of the J.P. Getty Foundation and the Andrew W. Mellon Foundation.

References

1. B. Newhall, *The History of Photography: From 1839 to the Present* (The Museum of Modern Art, New York, 1982)
2. L.-J.-M. Daguerre, *Historical and Descriptive Account of the Various Processes of the Daguerreotype and the Diorama* (Mc. Lean, London, 1839)
3. M.S. Barger, W.B. White, *The Daguerreotype. Nineteenth-Century Technology and Modern Science* (Johns Hopkins University Press, Baltimore, 1991)
4. G.B. Romer, B. Wallis, *Young America. The Daguerreotypes of Southworth & Hawes* (International Center of Photography/George Eastman House/Steidl Publishers, Rochester, Göttingen, 2005)
5. A. Swan, C.E. Fiori, K.F.J. Heinrich, Daguerreotypes: a study of the plates and the process. *Scanning Electron Microsc.* **1**, 411–424 (1979)
6. P. Ravines, A. West, J. Minter, R.O. Gutierrez Jr., The daguerreotype under high magnification: an ultra-high resolution SEM study of a 19th century daguerreotype's surface nanostructure, in *LASMAC 2009*, Cancun, Mexico (2009)
7. M.S. Barger, R. Messier, W.B. White, Gilding and sealing daguerreotypes. *Photogr. Sci. Eng.* **27**(4), 141–146 (1983)
8. E. Da Silva et al., Monitoring the photographic process, degradation and restoration of 21st century daguerreotypes by wavelength-dispersive X-ray fluorescence spectrometry. *J. Anal. At. Spectrom.* **25**(5), 654–661 (2010)
9. S.A. Centeno, T. Meller, N. Kennedy, M.T. Wypyski, The daguerreotype surface as a SERS substrate: characterization of image deterioration in plates from the 19th century studio of Southworth & Hawes. *J. Raman Spectrosc.* **39**(7), 914–921 (2008)
10. T.E. Graedel, Corrosion mechanisms for silver exposed to the atmosphere. *J. Electrochem. Soc.* **139**(7), 1963–1970 (1992)
11. A. Swan, The preservation of daguerreotypes, in *Annual Meeting of the American Institute for Conservation of Historic and Artistic Works* (The American Institute for Conservation of Historic and Artistic Works, Philadelphia, 1981)
12. C.V. Ravenswaay, An improved method for the restoration of daguerreotypes. *Image* **5**(7), 156–159 (1956)
13. M.S. Barger, S.V. Krishnaswamy, R. Messier, The cleaning of daguerreotypes: comparison of cleaning methods. *J. Am. Inst. Conserv.* **22**(1), 13–24 (1982)
14. I. Turovets, M. Maggen, A. Lewis, Cleaning of daguerreotypes with an excimer laser. *Stud. Conserv.* **43**(2), 89–100 (1998)
15. V.V. Golovlev, M.J. Gresalfi, J.C. Miller, D. Anglos, K. Melesanaki, V. Zafiropoulos, G. Romer, P. Messier, Laser characterization and cleaning of 19th century daguerreotypes II. *J. Cult. Heritage* **4**(Supplement 1), 134–139 (2003)
16. S.D. Humphrey, *American Hand Book of the Daguerreotype: Giving the Most Approved and Convenient Methods for Preparing the Chemicals and the Combinations Used in the Art. Containing the Daguerreotype, Electrotpe, and Various Other Processes Employed in Taking Helographic Impressions*, 5th edn. (S.D. Humphrey, New York, 1858)
17. F. Schulte, S.A. Centeno, A. Schrott, N.W. Kennedy, Characterization of chlorine induced alterations in daguerreotypes by SEM, XRF, and Raman spectroscopy, in *10th International Conference on Non-destructive Investigations and Microanalysis for the Diagnostics and Conservation of Cultural and Environmental Heritage (Art' 11)*, Florence (2011)
18. E.J. Liang, C. Engert, W. Kiefer, Surface-enhanced Raman-scattering of halide-ions, pyridine and crystal violet on colloidal silver with near-infrared excitation-low-wave-number vibrational-modes. *Vib. Spectrosc.* **8**(3), 435–444 (1995)
19. J.T. Zhang, X.L. Li, X.M. Sun, Y.D. Li, Surface enhanced Raman scattering effects of silver colloids with different shapes. *J. Phys. Chem. B* **109**(25), 12544–12548 (2005)

20. H. Sone et al., Nano-dots formation on silver sulphide surface using electron beam irradiation. *Microelectron. Eng.* **83**(4–9), 1487–1490 (2006)
21. Y.Y. Li, Y. Ding, Porous AgCl/Ag nanocomposites with enhanced visible light photocatalytic properties. *J. Phys. Chem. C* **114**(7), 3175–3179 (2010)
22. F. Moser, N.R. Nail, F. Urbach, Optical absorption studies of the volume photolysis of large silver chloride crystals. *J. Phys. Chem. Solids* **9**(3–4), 217–234 (1959)